Intermolecular Proton Binding in the Presence of a Large Electric Dipole: Ar-Tagged Vibrational Predissociation Spectroscopy of the $CH_3CN \cdot H^+ \cdot OH_2$ and $CH_3CN \cdot D^+ \cdot OD_2$ Complexes

George H. Gardenier, Joseph R. Roscioli, and Mark A. Johnson*

Sterling Chemistry Laboratory, Department of Chemistry, Yale University, P.O. Box 208107, New Haven, Connecticut 06520

Received: January 31, 2008; Revised Manuscript Received: June 20, 2008

We report Ar-predissociation vibrational spectra of the binary proton-bound hydrates of acetonitrile (AN), $AN \cdot H^+ \cdot OH_2$ and $AN \cdot D^+ \cdot OD_2$, in the 600−3800 cm^{-1} energy range. This complex was specifically chosen to explore the nature of the intermolecular proton bond when there is a large difference between the electric dipole moments of the two tethered molecules. Sharp, isotope-dependent bands in the vicinity of 1000 cm^{-1} are traced to $AN \cdot H^+ \cdot OH_2$ vibrations involving the parallel displacement of the shared proton along the heavy atom axis, $\nu_{sp}(\|)$. These transitions lie much lower in energy than anticipated by a recently reported empirical trend which found the $\nu_{sp}(\|)$ fundamentals to be strongly correlated with the difference in proton affinities (ΔPA) between the two tethered molecules (Roscioli et al., *Science,* **2007***, 316*, 249). The different behavior of the $AN \cdot H^+ \cdot OH_2$ complex is discussed in the context of the recent theoretical prediction (Fridgen, *J. Phys. Chem A.*, **2006,** *110*, 6122) that a large disparity in dipole moments would lead to such a deviation from the reported (ΔPA) trend.

I. Introduction

Two closed-shell molecules, A and B, each with a lone pair of electrons on an electronegative atom, can generally be held tightly together by their mutual attraction to an excess proton. The character of the resulting $A \cdot H^+ \cdot B$ intermolecular proton bond has recently been the focus of much attention as spectroscopists seek to identify the unique spectral signatures arising from the vibrational motion of the bridging proton.[1−8] Many earlier studies of these species in the condensed phase, as well as isolated in the form of gas-phase ions, suggested that the bands derived from the bridging proton were intrinsically diffuse because of strong coupling to the intramolecular vibrations in the two constituents.[7−11] Recently, however, we reported[1] Ar-tagging messenger predissociation spectra[12] of 19 gas-phase complexes (mostly combinations of hydrates, alcohols, and ethers) that displayed sharp bands, and the features derived from the shared-proton motion could be readily identified by using H/D isotopic substitution. Duncan and coworkers[13] have also obtained Ar photodissociation spectra of the protonated acetone dimer with similar results. Of the three vibrations expected for oscillation of the bridging proton, the fundamental arising from displacement along the heavy-atom axis ($\nu_{sp}(\|)$) was observed in all cases to carry the most oscillator strength. These $\nu_{sp}(\|)$ values appeared over a range of 2700 cm^{-1} in a manner that is strongly correlated with the difference between the proton affinities (ΔPA) of the two tethered molecules.

In a recent theoretical paper,[2] Fridgen explored how proton sharing was affected when there was a large difference between the electric dipole moments (μ) of the tethered molecules, which is a scenario not covered in our initial experimental survey.[1] Interestingly, he found that $A \cdot H^+ \cdot B$ complexes can adopt equilibrium structures in which the proton is preferentially associated with the molecule having the smaller (asymptotic) proton affinity (A) if the molecule with somewhat higher proton affinity (B) possesses a much larger dipole moment than that of the partner. This behavior was rationalized on the basis of intracluster electrostatic stabilization of the $\{AH^+ \cdots B\}$ configuration on the potential surface. Our goal here is to experimentally investigate this prediction by recording the predissociation spectrum of a proton-bound complex involving the acetonitrile molecule, AN, which has a significantly larger dipole moment (3.9 D) than those of the molecules canvassed in our first report (0 to 1.85 D).[1] Testing Fridgen's hypothesis requires choosing a partner molecule with smaller PA and lower dipole moment than those of AN, criteria which are met by the water molecule. The PA of AN is 88 kJ/mol higher than that of the water molecule, whereas the dipole moment of water (1.85 D) is about 2 D less than that of AN.[14] Ar-predissociation spectra are presented for the $AN \cdot H^+ \cdot OH_2 \cdot Ar$ and $AN \cdot D^+ \cdot OD_2 \cdot Ar$ isotopologues over the range 600−3800 cm^{-1}.

Vibrational assignments are aided by comparison with harmonic predictions[15] (MP2[16−19]/aug-cc-pVDZ[20−22] level), which are especially effective in identifying transitions associated with vibrations remote or uncoupled from the shared proton. It is becoming increasingly clear, however, from several recent examples (e.g., $H_3N \cdot H^+ \cdot NH_3$, $H_2O \cdot H^+ \cdot OH_2$, and the proton-bound dimer of dimethyl ether),[3,5,6,11,23−28] that the shared-proton vibrations appear far from the harmonic predictions because of both the anharmonicity of its potential surface as well as strong coupling with nearly iso-energetic vibrations nominally localized on the molecular constituents.[1,8,11] Accurate theoretical treatment of even the simplest complexes has proven to be nontrivial. For example, a fully anharmonic (15-dimensional) calculation was required to recover the rather simple band pattern observed in $H_5O_2^+$.[26] It is useful, therefore, to experimentally establish the locations of bands mostly associated with the bridging proton displacement by using isotope shifts combined with estimates

* To whom correspondences should be addressed. E-mail: mark.johnson@yale.edu.

10.1021/jp800948s CCC: $40.75
Published on Web 11/04/2008

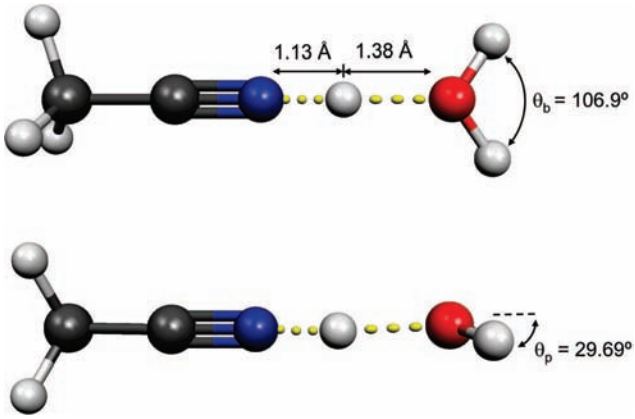

Figure 1. Two perspective views of the AN·H$^+$·OH$_2$ minimum-energy structure (MP2/aug-cc-pVDZ level) with key structural parameters indicated.

of the shared proton fundamental, where the anharmonic nature of the trapping potential along the heavy-atom axis is treated with a one-dimensional approach.[1,29,30]

The (MP2/aug-cc-pVDZ level) ab initio minimum-energy structure for the AN·H$^+$·OH$_2$ complex is shown in Figure 1 along with values of several key structural parameters. Note that the shared proton is closer to the N atom, as anticipated from the higher PA of AN, but observe that the axis of the water molecule is tilted (θ_p, lower structural view in Figure 1) off of the NO axis by about 30°. The water molecule also exhibits 1% elongation of the OH bond and 2% opening of the HOH bond angle (θ_b, upper structural view in Figure 1) upon complexation. Together, these distortions are consistent with partial relaxation of the molecular framework toward that of pyramidal H_3O^+. Of course, the infrared spectra of interest here are a consequence of the vibrationally averaged, high-amplitude motion characteristic of the shared proton and thus explore extended regions of the potential energy surface.

II. Experimental Details

Mass-selected vibrational predissociation spectra were obtained with the Ar-tagging method[12] by using the Yale double-focusing, tandem time-of-flight (TOF) photofragmentation spectrometer described previously.[31] The AN·H$^+$·OH$_2$ and AN·D$^+$·OD$_2$ clusters were synthesized by using Ar-mediated proton-transfer chemistry in the supersonic ion source. This typically involved seeding trace water vapor in an Ar expansion (general valve, 0.5 mm nozzle, Parker-Hannifin) ionized with a pulsed (50 microseconds), 1 keV counterpropagating electron beam.

The ionization procedure outlined above generates large quantities of the argon-solvated Zundel ion clusters, $H_5O_2^+ \cdot Ar_n$, which are then converted to the required AN·H$^+$·OH$_2$ complexes, presumably through the ligand-switching reaction:

$$AN + H_2O \cdot H^+ \cdot OH_2 \cdot Ar_m \rightarrow AN \cdot H^+ \cdot OH_2 \cdot Ar_p + H_2O + (m-p)Ar \quad (1)$$

The reaction was carried out by entraining AN into the supersonic expansion at low pressure through an independently timed pulsed valve.[32] The AN·H$^+$·OH$_2$·Ar$_p$ clusters were mass-selected prior to their characterization by vibrational predissociation spectroscopy

$$AN \cdot H^+ \cdot OH_2 \cdot Ar_p + h\nu \rightarrow AN \cdot H^+ \cdot OH_2 + pAr \quad (2)$$

for $p = 1$ and 2. This technique[12] has two significant advantages in that (i) the Ar-tagged complexes are necessarily internally cold and (ii) the resulting spectra are recorded in a linear (one-photon) action regime. However it also introduces the complication that Ar attachment perturbs the structure of the ion.[3,25,33] The two advantages often outweigh the complication of perturbation, because Ar-tagged spectra are much simpler than those obtained for the same (bare) complexes by using multiple photon dissociation.[5,8,34] We present the results for tagging with one and two Ar atoms to empirically gauge the extent of perturbation caused in this case. Infrared excitation was carried out with a 10 ns, 10 Hz Nd:YAG-pumped OPO/OPA laser system (LaserVision) which generates IR light in the 600−4400 cm^{-1} range by using three stages of parametric conversion (KTP/KTA/AgGaSe$_2$).[35,36]

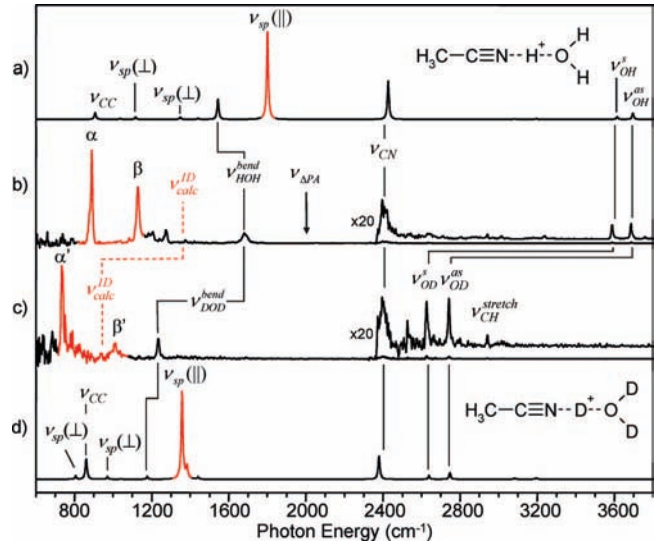

Figure 2. (a) Calculated harmonic spectrum of AN·H$^+$·OH$_2$, (b) experimental predissociation spectrum of AN·H$^+$·OH$_2$·Ar, (c) experimental predissociation spectrum of AN·D$^+$·OD$_2$·Ar, and (d) calculated harmonic spectrum of AN·D$^+$·OD$_2$. Harmonic values for water-based vibrations are scaled (see Table 1 footnote for specifics). Calculated transitions dominated by parallel displacements of the shared protons (ν_{sp}(||)) are highlighted in red, whereas group vibrations remote from the excess proton are indicated according to largest displacements in the normal modes. The bands labeled $\nu_{sp}(\perp)$ indicate the two harmonic transitions arising from displacement of the proton perpendicular to the heavy atom axis. The solid arrow labeled $\nu_{\Delta PA}$ in (b) indicates the expected[1] position of ν_{sp}(||) based upon the difference between the proton affinities of AN and H_2O. The dashed red line indicates predicted ν_{sp}(||) transitions obtained by using numerical solutions to the 1-D Schrödinger equation for the MP2/aug-cc-pVDZ potential energy surface shown in Figure 3. Peaks labeled α and β in trace b indicate isotope-dependent transitions assigned to ν_{sp}(||) activity in AN·H$^+$·OH$_2$, whereas peak α′ appears mostly associated with ν_{sp}(||) in AN·D$^+$·OD$_2$.

III. Results and Discussion

III.A. Ar-Tagged Spectra of the AN·H$^+$·H$_2$O and AN·D$^+$·D$_2$O Complexes: Assignment of the Bridging Proton Fundamental Excitation Energies by Using Isotope Shifts and 1-D Anharmonic Calculations. Figure 2 presents the observed predissociation spectra for AN·H$^+$·OH$_2$·Ar (Figure 2b) and AN·D$^+$·OD$_2$ ·Ar (Figure 2c) along with the harmonic predictions for the structure displayed in Figure 1 in the upper (Figure 2a) and lower traces (Figure 2d). Most of the weaker transitions are readily assigned to the intramolecular motions of the AN and water molecules. In particular, the two bands highest in energy are due to the symmetric (ν^s) and asymmetric (ν^{as}) OH (or OD) stretching normal modes, whereas the intramolecular bending motions of the water molecule (ν^{bend})

TABLE 1: Energies (cm^{-1}) of Observed[a] Vibrational Predissociation Transitions for the AN Complexes $AN\cdot H^+\cdot H_2O\cdot Ar$ and $AN\cdot H^+\cdot D_2O\cdot Ar$, with Calculated[b] Fundamentals for the Bare (non-Ar-tagged) Analogues in Parentheses[c]

vibrational mode	$AN\cdot H^+\cdot H_2O$		$AN\cdot D^+\cdot D_2O$	
$\nu_{sp}(\|\|)$	$1130^{d,\beta}$	(1802, 1365^e)	$738^{d,\alpha'}$	(1359, 942^e)
ν_{CC}^{s}	$890^{d,\alpha}$	(907)	$1006^{d,\beta'}$	(861)
ν_{HOH}^{bend}	1679	$(1540)^f$	1236	$(1175)^f$
$\nu_{CN}^{stretch}$	2405	(2427)	2402	(2380)
ν_{CH}^{s}	2943	(3083)	2941	(3083)
ν_{OH}^{s}	3590	$(3608)^f$	2626	$(2628)^f$
ν_{OH}^{as}	3686	$(3720)^f$	2742	$(2757)^f$

[a] Experimental values accurate to ±5 cm^{-1}. [b] Numbers in parentheses indicate harmonic values at MP2/aug-cc-pVDZ level/basis. [c] Vibrational modes are designated according to the largest displacements in the calculated normal modes. [d] Both transitions (α and β in Figure 2b) are quenched upon H/D substitution and are tentatively assigned to a mixed set of levels arising from coupling between $\nu_{sp}(\|)$ and ν_{CC}^{s}. [e] 1-D anharmonic value based on numerical integration of the potential shown in Figure 3. [f] Factors for scaled harmonic values at MP2/aug-cc-pVDZ determined by comparing the calculated frequencies in the neutral H_2O and D_2O molecules to their experimental values[37] as follows: HOH bend, 0.98; DOD bend, 0.99; OH stretch, 0.96; OD stretch, 0.99.

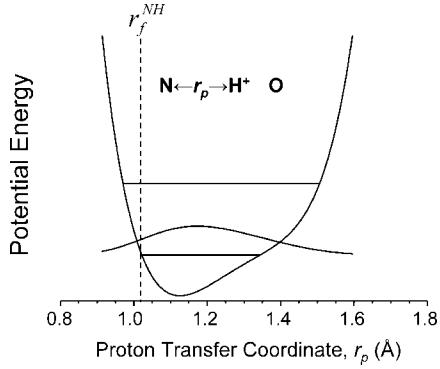

Figure 3. Calculated potential energy surface (MP2/aug-cc-pVDZ) for displacement of the bridging proton with all other atoms fixed at the minimum-energy $AN\cdot H^+\cdot OH_2$ structure. The zero-point wave function and energy levels for the first two states of the asymmetric proton stretch, $\nu_{sp}(\|)$, are included. The calculated N−H bond length in protonated AN is indicated by the dashed line.

can be unambiguously assigned to uncluttered transitions at 1679 and 1236 cm^{-1} for H_2O and D_2O, respectively. The weaker CH stretches at 2941 cm^{-1} appear close to their locations in the isolated AN molecule (2954 cm^{-1}).[37] On the other hand, the substantial blue shift of the nominally CN stretching feature, which occurs at 2405 cm^{-1} in the complex compared to 2267 cm^{-1} in isolated AN, is anticipated at the harmonic level.[38] The observed and calculated band positions are collected in Table 1.

The strongest transitions in the calculated spectra (1802 in Figure 2a and 1359 in Figure 2d) are associated with modes having the largest parallel displacements of the shared proton ($\nu_{sp}(\|)$), and these appear much higher in energy than the most intense features in the experimental spectra. In particular, two intense features in the light isotopomer around 1000 cm^{-1} (denoted α and β in Figure 2b) are quenched in the $AN\cdot D^+\cdot OD_2$ isotopologue (Figure 2c), indicating that both involve the motion of the shared proton.

Assignment of the strong, isotope-dependent bands (α and β in Figure 2b) to activity in the $\nu_{sp}(\|)$ fundamental transition is aided by consideration of the calculated potential for 1-D shared-proton displacement, with the N−O distance frozen at the equilibrium geometry of the complex.[39,40] The potential curve obtained at the MP2/aug-cc-pVDZ level[1,41] is presented in Figure 3. Although the minimum-energy configuration of the $AN\cdot H^+\cdot OH_2$ complex does indeed attach the proton closer to the N atom, there is a pronounced shelf in the potential at an NH bond length of ∼1.4 Å, which corresponds to the $AN\cdots H^+OH_2$ configuration.

Within the 1-D approximation, one can roughly estimate the $\nu_{sp}(\|)$ transition energies by numerically solving the Schrödinger equation for the potential displayed in Figure 3.[42,43] The ground-state vibrational wave function is included in Figure 3, along with the first two energy levels. The resulting transition energies are listed in Table 1 and are indicated by the dashed line labeled ν_{calc} in Figure 2. The predicted 1365 cm^{-1} value for $AN\cdot H^+\cdot OH_2$ is much closer to the observed α and β bands in Figure 2b than is the harmonic prediction. Given the crude level of the 1-D analysis, we are confident in the assignment of the features highlighted red in Figure 2b to vibrations deriving their oscillator strength from the $\nu_{sp}(\|)$ fundamental transitions. Interestingly, the $\nu_{sp}(\|)$ value in $AN\cdot H^+\cdot OH_2$ occurs in the same energy range where we have typically found it in symmetrical (e.g., $H_2O\cdot H^+\cdot OH_2$, the proton-bound dimer of dimethyl ether, etc.) complexes.[1]

The 1-D treatment obviously cannot explain the fact that two transitions (α and β in Figure 2b) are quenched upon deuteration. There are two perpendicular vibrations of the bridging proton ($\nu_{sp}(\perp)$) with harmonic values in the 1000 cm^{-1} range, but they are predicted to be much less intense than that mostly based on $\nu_{sp}(\|)$. It is significant that many of the complexes studied earlier[1] similarly displayed two or more intense bands near 1000 cm^{-1} that were strongly isotope dependent. This effect has been considered in a very recent theoretical paper[11] discussing the mixing of nominally $\nu_{sp}(\|)$ motion with near-resonant vibrations of the attached molecules in the protonated dimethyl ether dimer. In that case, several of the resulting delocalized modes that involve parallel proton displacement dominate the spectrum. In many respects, this mixing can be viewed as a dilution of the intrinsically large $\nu_{sp}(\|)$ oscillator strength into the background states of the complex. When the resonance is broken by H/D substitution, the mixing is suppressed, and thus, several transitions are affected upon deuteration. In the present case, the CC-stretching vibration of the AN molecule (920.3 cm^{-1})[44] likely plays a significant role in the strong transitions at 890 and 1130 cm^{-1} in $AN\cdot H^+\cdot OH_2$.

Given the advanced level of theory required to solve the multidimensional vibrational level structure in simpler systems (e.g., $H_5O_2^+$, $H_7N_2^+$),[6,26] it is appropriate in this experimental study to focus on the spectral range of $\nu_{sp}(\|)$ activity for comparison with the trend in ΔPA established previously.[1] In this context, the most important result of this work is that the $\nu_{sp}(\|)$-based transitions in the $AN\cdot H^+\cdot OH_2$ complex (α and β in Figure 2b) occur about 900 cm^{-1} lower than those displayed by the systems reported earlier with similar ΔPA. As a specific example to emphasize the point, the ethanol·H^+·water complex, with a comparable ΔPA (= 85 kJ/mol vs 88 kJ/mol for $AN\cdot H^+\cdot OH_2$) has a $\nu_{sp}(\|)$ value of 1964 cm^{-1}, almost twice that displayed by the shared proton activity in the protonated AN monohydrate. The value anticipated from the earlier ΔPA trend is indicated by the solid arrow in Figure 2b (labeled $\nu_{\Delta PA}$), which occurs in a completely quiet region of the spectrum.

This break of the observed $AN\cdot H^+\cdot OH_2$ behavior with that of the previously studied[1] systems is consistent with the prediction by Fridgen.[2] Presumably, the dipole effect emphasized

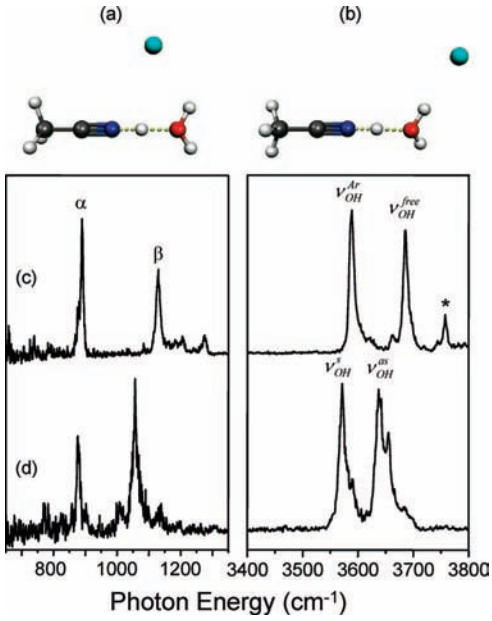

Figure 4. Two minimum-energy configurations of the $AN\cdot H^+\cdot OH_2\cdot Ar$ complex with the Ar atom attached (a) above the shared proton and (b) to the dangling OH group on the water molecule. Argon predissociation spectra of (c) $AN\cdot H^+\cdot OH_2\cdot Ar$ and (d) $AN\cdot H^+\cdot OH_2\cdot Ar_2$. Assignments of the major peaks are included as in Figure 2. The peak labeled * often occurs in protonated hydrates, and likely arises from a combination band involving a soft mode of the complex.

in that work would act to lower the $\nu_{sp}(II)$ frequency, as we observe, by flattening the shared-proton potential in the region of the $AN\cdots H_3O^+$ configuration (shelf in Figure 3). Although it remains to be determined whether the magnitude of the observed difference can be generally correlated with the asymptotic dipole moments, the search for such a trend is clearly warranted in light of the present observation.

III.B. Evaluation of Ar Perturbation by Comparison of the $AN\cdot H^+\cdot OH_2\cdot Ar_m$, $m = 1$ and 2 Clusters. An important limitation of the Ar-tagging method is, of course, that the attached Ar atom perturbs the complex.[3,25] One way to experimentally address the extent of the perturbation is to monitor how the spectrum changes upon sequential addition of Ar atoms,[3,25] because the magnitude of the incremental band shifts often reflects the scale of the perturbation.[33,45] We therefore acquired the spectra of the $AN\cdot H^+\cdot OH_2\cdot Ar_p$, $p = 1$ and 2 species with the results presented in Figure 4. The behavior of the free OH-stretching bands is most informative, because the second Ar atom yields a significant (49 cm^{-1}) red shift in the upper of the two strong bands arising from the OH stretches. The addition of Ar to a dangling OH group of a water molecule generally induces a red shift,[25] effectively decoupling the symmetric and antisymmetric OH stretches into a free and an Ar-bound stretch, as indicated by the superscripts in the labels of the strong OH-stretching bands near 3650 cm^{-1} in the $p = 1$ spectrum shown in Figure 4c. We therefore infer that the first Ar atom is already attached to one of the H atoms on the water molecule, accounting for the lower-energy OH-stretching band, whereas the second Ar attaches to the remaining free OH, thus explaining the observed red shift of the higher-energy OH-stretching band in $AN\cdot H^+\cdot OH_2\cdot Ar_2$.

We also carried out electronic structure calculations[15] (MP2/aug-cc-pVDZ level/basis) to identify plausible Ar binding sites and recovered the two local minima shown in the insets at the top of Figure 4. One of these has the Ar attached closer to the shared proton (Figure 4a), whereas in the other, the Ar atom binds to a dangling OH group (Figure 4b). There is precedent for both in the literature,[3,13,46] and in this case, the OH-bound structure is calculated to lie lowest in energy by ~65 cm^{-1} after zero-point corrections. As discussed in the previous paragraph, the spectra are consistent with preferential attachment to the dangling OH groups, which is the strongly preferred arrangement in Ar attachment to the related $H_5O_2^+$ ion.[25]

The Ar-solvation behavior of the strong bands near 1000 cm^{-1} associated with the shared proton are shown in Figure 4d. The most important aspect of this Ar-dependent study is that these $\nu_{sp}(II)$-based bands are not strongly perturbed by solvation. The basic effect is that the higher energy band near 1130 cm^{-1} in the single Ar case is red-shifted by about 65 cm^{-1}, whereas the lower energy feature at 890 cm^{-1} is much less affected with a red shift of only 5 cm^{-1}. Interestingly, the direction of the solvent shift is opposite to that displayed by the $\nu_{sp}(II)$ bands in $H_5O_2^+$, where the addition of Ar acts to break the symmetry of the complex and pull the proton toward the water molecule to which the Ar atoms are attached.[3] This different behavior of the asymmetric $AN\cdot H^+\cdot OH_2$ complex can be rationalized if the degree of asymmetry is reduced upon Ar attachment to the water (by again increasing its PA), thus creating a condition of more equal sharing with a concomitant lowering of the $\nu_{sp}(II)$ value. Note that these perturbations are minor effects, however, and do not complicate the main observation that the $\nu_{sp}(II)$ value observed in the $AN\cdot H^+\cdot OH_2$ system falls far below the trend expected from the difference in PA of the constituents.

IV. Summary

We report Ar-predissociation spectra of the proton-bound monohydrate of AN. The H/D isotope dependence of the bands enables the assignment of two strong transitions in the 1000 cm^{-1} region to vibrations involving the motion of the shared proton along the heavy atom axis. The location of the $\nu_{sp}(II)$ transition falls about 900 cm^{-1} lower in energy than anticipated by the trend reported earlier, where the $\nu_{sp}(II)$ values were observed to be strongly correlated with the difference in proton affinities (ΔPA) of the two flanking molecules.[1] This behavior is in qualitative agreement with the theoretical prediction of Fridgen,[2] who anticipated this break with the ΔPA trend in the context of AN's large electric dipole moment.

Acknowledgment. We thank the experimental chemistry division of the National Science Foundation, supplemented by the NSF "Fueling the Future" Chemical Bonding Center, for support of this work.

References and Notes

(1) Roscioli, J. R.; McCunn, L. R.; Johnson, M. A. *Science* **2007**, *316*, 249.

(2) Fridgen, T. D. *J. Phys. Chem. A* **2006**, *110*, 6122.

(3) Hammer, N. I.; Diken, E. G.; Roscioli, J. R.; Johnson, M. A.; Myshakin, E. M.; Jordan, K. D.; McCoy, A. B.; Huang, X.; Bowman, J. M.; Carter, S. *J. Chem. Phys.* **2005**, *122*, 244301.

(4) Fridgen, T. D.; MacAleese, L.; McMahon, T. B.; Lemaire, J.; Maitre, P. *Phys. Chem. Chem. Phys.* **2006**, *8*, 955.

(5) Asmis, K. R.; Pivonka, N. L.; Santambrogio, G.; Brümmer, M.; Kaposta, C.; Neumark, D. M.; Wöste, L. *Science* **2003**, *299*, 1375.

(6) Asmis, K. R.; Yang, Y. G.; Santambrogio, G.; Brummer, M.; Roscioli, J. R.; McCunn, L. R.; Johnson, M. A.; Kuhn, O. *Angew. Chem., Int. Ed.* **2007**, *46*, 8691.

(7) Fridgen, T. D.; MacAleese, L.; Maitre, P.; McMahon, T. B.; Boissel, P.; Lemaire, J. *Phys. Chem. Chem. Phys.* **2005**, *7*, 2747.

(8) Moore, D. T.; Oomens, J.; van der Meer, L.; von Helden, G.; Meijer, G.; Valle, J.; Marshall, A. G.; Eyler, J. R. *Chem. Phys. Chem.* **2004**, *5*, 740.

(9) Stoyanov, E. S.; Reed, C. A. *J. Phys. Chem. A* **2006**, *110*, 12992.

(10) Zundel, G. *Adv. Chem. Phys.* **2000**, *111*, 1.

(11) Li, X.; Moore, D. T.; Iyengar, S. S. *J. Chem. Phys.* **2008**, *128*, 184308.

(12) Okumura, M.; Yeh, L. I.; Myers, J. D.; Lee, Y. T. *J. Chem. Phys.* **1986**, *85*, 2328.

(13) Douberly, G. E.; Ricks, A. M.; Ticknor, B. W.; Duncan, M. A. *Phys. Chem. Chem. Phys.* **2008**, *10*, 77.

(14) Hunter, E. P.; Lias, S. G. Proton Affinity Evaluation. In *NIST Chemistry WebBook, NIST Standard Reference Database Number 69*; Linstrom, P. J., Mallard, W. G. Eds.; National Institute of Standards and Technology: Gaithersburg, MD, June 2005.

(15) Firsch, M. J.; Trucks, G. W.; Schiegel, H. B.; Scuseria, G. E.; Robb, M. A.; Cheeseman, J. R.; Jr. J. A. M.; Vreven, T.; Kudin, K. N.; Burant, J. C.; Millam, J. M.; Lyengar, S. S.; Tomasi, J.; Barone, V.; Mennucci, B.; Cossi, M.; Scalmani, G.; Rega, N.; Petersson, G. A.; Nakatsuji, H.; Hada, M.; Ehara, M.; Toyota, K.; Fukuda, R.; Haseqawa, J.; Ishida, M.; Nakajima, T.; Honda, Y.; Kitao, O.; Nakai, H.; Klene, M.; Li, X.; Knox, J. E.; Hratchian, H. P.; Cross, J. B.; Vakken, B.; Adamo, C.; Jaramillo, J.; Gomperts, R.; Stratmann, R. E.; Yazyev, O.; Austin, A. J.; Cammi, R.; Pomelli, C.; Ochterski, J. W.; Ayala, P. Y.; Morokuma, K.; Voth, G. A.; Salvador, P.; Dannenberg, J. J.; Zakrzewski, V. G.; Dapprich, S.; Daniels, A. D.; Strain, M. C.; Farkas, O.; Malick, D. K.; Rabuck, A. D.; Raghavachari, K.; Foresman, J. B.; Ortiz, J. V.; Cui, Q.; Baboul, A. G.; Clifford, S.; Coisiowski, J.; Stefanov, B. B.; Liu, G.; Liashenko, A.; Piskorz, P.; Komaromi, I.; Martin, R. L.; Fox, D. J.; Keith, T.; Al-Laham, M. A.; Peng, C. Y.; Nanayakkara, A.; ChallacombeM. Gill, P. M. W.; Johnson, B.; Wong, M. W.; Gonzales, C.; Pople, J. A.; *Gaussian 03, Revision C.02*; Gaussian, Inc.: Wallingford, CT, 2004.

(16) Frisch, M. J.; Head-Gordon, M.; Pople, J. A. *Chem. Phys. Lett.* **1990**, *166*, 275.

(17) Frisch, M. J.; Head-Gordon, M.; Pople, J. A. *Chem. Phys. Lett.* **1990**, *166*, 281.

(18) Pople, J. A.; Krishana, R.; Schielgel, H. B.; Binkley, J. S. *Int. J. Quantum Chem. Symp.* **1979**, *13*, 325.

(19) Handy, N. C.; Schaefer, H. F. *J. Chem. Phys.* **1984**, *81*, 5031.

(20) Dunning, T. H. *J. Chem. Phys.* **1989**, *90*, 1007.

(21) Kendall, R. A.; Dunning, T. H. Jr.; Harrison, R. J. *J. Chem. Phys.* **1992**, *96*, 6796.

(22) Woon, D. E.; Dunning, T. H. Jr. *J. Chem. Phys.* **1993**, *98*, 1358.

(23) Headrick, J. M.; Bopp, J. C.; Johnson, M. A. *J. Chem. Phys.* **2004**, *121*, 11523.

(24) Diken, E. G.; Headrick, J. M.; Roscioli, J. R.; Bopp, J. C.; Johnson, M. A.; McCoy, A. B. *J. Phys. Chem. A* **2005**, *109*, 1487.

(25) McCunn, L. R.; Roscioli, J. R.; Johnson, M. A.; McCoy, A. B. *J. Phys. Chem. B* **2008**, *112*, 321.

(26) Vendrell, O.; Gatti, F.; Meyer, H.-D. *J. Chem. Phys.* **2007**, *127*, 184303.

(27) Dai, J.; Bacic, Z.; Huang, X.; Carter, S.; Bowman, J. M. *J. Chem. Phys.* **2003**, *119*, 6571.

(28) Kaledin, M.; Kaledin, A. L.; Bowman, J. M. *J. Phys. Chem. A* **2006**, *110*, 2933.

(29) Xie, Y. M.; Remington, R. B.; Schaefer, H. F. *J. Chem. Phys.* **1994**, *101*, 4878.

(30) Kim, K. S. *J. Chem. Phys.* **2000**, *113*, 5259.

(31) Posey, L. A.; Johnson, M. A. *J. Chem. Phys.* **1988**, *89*, 4807.

(32) Robertson, W. H.; Kelley, J. A.; Johnson, M. A. *Rev. Sci. Instrum.* **2000**, *71*, 4431.

(33) Corcelli, S. A.; Kelley, J. A.; Tully, J. C.; Johnson, M. A. *J. Phys. Chem. A* **2002**, *106*, 4872.

(34) Fridgen, T. D.; McMahon, T. B.; MacAleese, L.; Lemaire, J.; Maitre, P. *J. Phys. Chem. A* **2004**, *108*, 9008.

(35) Gerhards, M.; Unterberg, C.; Gerlach, A. *Phys. Chem. Chem. Phys.* **2002**, *4*, 5563.

(36) Stearns, J. A.; Das, A.; Zwier, T. S. *Phys. Chem. Chem. Phys.* **2004**, *6*, 2605.

(37) Shimanouchi, T. Molecular Vibrational Frequencies. In *NIST Chemistry WebBook, NIST Standard Reference Database*; Mallard, W. G., Linstrom, P. J. Eds.; National Institute of Standards and Technology: Gaithersburg, MD, June 2005; Vol. 69, http://webbook.nist.gov.

(38) Suzuki, I.; Nakagawa, J.; Fujiyama, T. *Spectrochim. Acta* **1977**, *33A*, 689.

(39) Kim, J.; Lee, H. M.; Suh, S. B.; Majumdar, D.; Kim, K. S. *J. Chem. Phys.* **2000**, *113*, 5259.

(40) Yates, B. F.; Schaefer, H. F., III; Lee, T. J.; Rice, J. E. *J. Am. Chem. Soc.* **1988**, *110*, 6327.

(41) Roscioli, J. R.; Diken, E. G.; Johnson, M. A.; Horvath, S.; McCoy, A. B. *J. Phys. Chem. A* **2006**, *110*, 4943.

(42) Yates, B. F.; Schaefer, H. F.; Lee, T. J.; Rice, J. E. *J. Am. Chem. Soc.* **1988**, *110*, 6327.

(43) Kim, J.; Lee, H. M.; Suh, S. B.; Majumdar, D.; Kim, K. S. *J. Chem. Phys.* **2000**, *113*, 5259.

(44) Parker, F. W.; Nielsen, A. H.; Flethcher, W. H. *J. Mol. Spectrosc.* **1957**, *1*, 107.

(45) Neilsen, S. B.; Ayotte, P.; Kelley, J. A.; Johnson, M. A. *J. Chem. Phys.* **1999**, *111*, 9593.

(46) Douberly, G. E.; Ricks, A. M.; Ticknor, B. W.; Duncan, M. A. *J. Phys. Chem. A* **208**, *112*, 950.

JP800948S